Size dependence of magnetic switching in perpendicularly magnetized MgO/Co/Pt pillars close to the spin reorientation transition

W. Stefanowicz,[1,2,a)] L. E. Nistor,[1,2,b)] S. Pizzini,[1,2] W. Kuch,[3] L. D. Buda-Prejbeanu,[4] G. Gaudin,[4] S. Auffret,[4] B. Rodmacq,[4] and J. Vogel[1,2,c)]
[1]*CNRS, Institut Néel, 38042 Grenoble, France*
[2]*Institut Néel, Univ. Grenoble Alpes, 38042 Grenoble, France*
[3]*Institut für Experimentalphysik, Freie Universität Berlin, Arnimallee 14, 14195 Berlin, Germany*
[4]*SPINTEC, UMR 8191, CEA/CNRS/UJF/Grenoble-INP, INAC, 38054 Grenoble, France*

(Received 19 September 2013; accepted 16 December 2013; published online 8 January 2014)

We investigated the magnetic switching of MgO/Co/Pt pillars with perpendicular magnetic anisotropy, for lateral pillar sizes from 30 nm to 2 μm and for Co layer thicknesses between 1.8 and 2.6 nm. For large pillars, both the coercivity and the remanent magnetization decrease for increasing Co thickness. For all Co thicknesses, the coercivity strongly increases upon decreasing the pillar size. A comparison with micromagnetic simulations shows that the change in coercivity is determined by size-dependent demagnetizing effects. Our results show that small pillars with perpendicular magnetization and a tunable coercivity can be fabricated from continuous layers with in-plane magnetization. © *2014 AIP Publishing LLC*. [http://dx.doi.org/10.1063/1.4860985]

Oxide/ferromagnetic metal (FM)/Normal metal (Pt,Ta) trilayered structures where the FM layer has a perpendicular magnetic anisotropy (PMA)[1] are important building blocks for the fabrication of perpendicular magnetic tunnel junctions (MTJ).[2] Although the magnetic properties and magnetization switching in continuous layers and nanostructures with perpendicular magnetization have been widely studied, most of these studies have been performed on materials with strong PMA like Co/Pt multilayers[3] and Co/Pd multilayers,[4] where the PMA originates from interface anisotropy, and CoPt[5] and FePt $L1_0$ ordered alloys,[6–8] where the bulk magneto-crystalline anisotropy causes the PMA. The strong PMA in these materials allows good stability against thermal agitation when the lateral sizes are reduced and makes them promising for high density data storage, but their electronic transport properties make them less adapted for use in MTJ. For this purpose, direct contact between the magnetic layer and an oxide is needed, which explains the large increase in the research on perpendicular MTJ after the discovery of perpendicular interfacial magnetic anisotropy at certain interfaces between a ferromagnetic layer and an oxide.[1,2,9] In this case, the interfacial PMA is relatively small and the magnetization orientation depends on the competition between the interfacial PMA and the demagnetizing energy, which favors in-plane magnetization. This competition depends both on the FM layer thickness and the lateral size of the MTJ element.

Several groups have studied the current-induced magnetization reversal of Oxide/FM/Normal metal-based MTJs with perpendicular magnetization, for pillars with different lateral sizes. In most cases, the switching current density was found to be independent of the pillar area, while the thermal activation for switching was proportional to the area up to lateral sizes of 50–100 nm, above which it was approximately constant. This was attributed to a change in magnetization reversal mechanism, from coherent rotation for small pillars to domain nucleation and domain wall propagation for larger pillars.[10–12] In some cases, an increase of the switching current density was found for small pillars, which was attributed to an increase of the perpendicular anisotropy due to demagnetizing effects.[13] Ref. 13 also showed a proportionality between the coercivity of the soft magnetic layer, measured from hysteresis loops using a magnetic field, and the critical current density for current-induced switching. Since magnetic field studies do not require electrical contacting of the individual pillars, they allow characterizing rapidly a large number of pillar sizes and Co thicknesses. They can thus be used for tuning the thickness of the magnetic layer and the size of the pillar, in order to optimize the trade-off between thermal stability and critical current density for spin-transfer torque (STT) switching.[14,15]

In this Letter, we report on a systematic investigation of field-induced magnetization switching in MgO/Co/Pt pillars with Co thicknesses between 1.8 and 2.6 nm, and lateral sizes between 30 nm and 2 μm. This Co thickness range is around the spin reorientation transition, where in the continuous layers the preferred orientation of the magnetization changes from out-of-plane to in-plane when the Co thickness increases. For each Co thickness, we observe a strong increase of the coercivity upon decreasing the pillar size. Micromagnetic simulations confirm that this increase of coercivity can be attributed to the dependence of demagnetizing effects on the pillar size.

MgO/Co(t)/Pt(2)/Ta(3)/Si layers (thickness in nm) were prepared by dc-sputtering onto thermally oxidized Si substrates. A 1.4 nm thick Mg layer was deposited and oxidized under partial O_2 atmosphere in order to obtain the MgO layer. The samples were annealed at 280 °C in order to activate the Co-O bond formation at the Co/MgO interface leading to the interfacial anisotropy.[16,17] They were protected from further oxidation by a cover layer of 2 nm of Pt.

[a)]Present address: Institute of Physics, Polish Academy of Sciences, al. Lotników 32/46, 02-668 Warszawa, Poland.
[b)]Present address: Applied Materials, Inc., Meylan, France.
[c)]Electronic mail: jan.vogel@neel.cnrs.fr.

Nanopatterning was performed by electron-beam lithography using a negative resist and ion beam etching techniques. Areas of $10 \times 10\,\mu m^2$ with pillar diameters of 30, 60, 140, 200, 300, and 500 nm, and 1 and 2 μm were fabricated. The spacing between pillars was 500 nm for the largest pillars, while for the 30, 60, and 140 nm pillars arrays with spacings of 40, 90, 190, and 490 nm were prepared (Fig. 1).

In order to estimate the magnetic anisotropy as a function of Co thickness, we recorded magnetic hysteresis loops on the continuous layers using extraordinary Hall effect (EHE) measurements, for both in-plane and out-of-plane magnetic fields. The dependence of the coercive field on Co thickness and pillar size was measured using a focused Kerr magnetometer with a smallest laser spot size of $0.8 \times 1.2\,\mu m^2$. Hysteresis loops were acquired with the magnetic field applied perpendicular to the film plane, using two different electromagnets, one with a maximum field of 80 mT and a remanence lower than 1 mT, another one with a higher maximum field of 125 mT and a remanence of about 9 mT. The magnetic signal was integrated over the laser spot, meaning that for pillar sizes smaller than the laser spot size the hysteresis loops contain the contributions of a number of pillars. For a more accurate determination of the value of the spontaneous magnetization, magnetic measurements were performed on continuous films using a commercial Superconducting Quantum Interference Device (SQUID) MPMS 5XL from Quantum Design. The size of the pillars and the spacing between them was verified using scanning electron microscopy (SEM).

Representative EHE loops for three different Co thicknesses (2.02 nm, 2.18 nm, and 2.47 nm), for an out-of-plane magnetic field, are shown in Fig. 2. These loops show that the out-of-plane remanence is 100% for 2.02 nm of Co, while it is about 60% for 2.18 nm and close to 0% for 2.47 nm of Co. The effective anisotropy K_{eff} is determined by taking the difference between the areas above magnetization curves measured along hard and easy magnetic axes.[18] K_{eff} is given by $K_{eff} = K_V + (K_{MgO} + K_{Pt})/t - (\mu_0 M_S^2/2)$, where K_V is the Co bulk anisotropy, and K_{MgO} and K_{Pt} are the contributions of the Co/MgO and Co/Pt interfaces to the anisotropy, respectively. $\mu_0 M_S^2/2$ is the demagnetizing energy for a continuous layer, which is modified when going to small pillars. The thickness dependence of $K_{eff} \times t$ is given in Fig. 3, showing that the transition from out-of-plane ($K_{eff} > 0$) to in-plane magnetization ($K_{eff} < 0$) takes place close to a Co thickness of 2.18 nm, where $K_{eff} = 0.9 \times 10^4\,J/m^3$. A linear fit to the data shows that $K_{MgO} + K_{Pt} = (3.1 \pm 0.1) \times 10^{-3}\,J/m^2$,

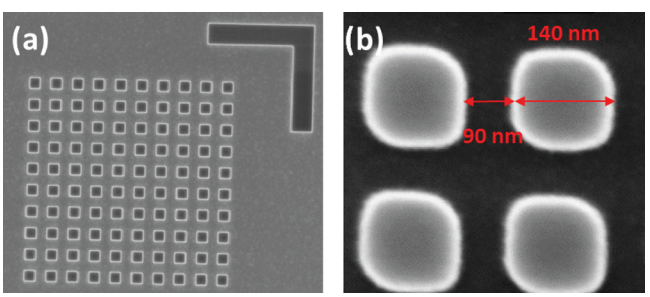

FIG. 1. (a) SEM image of 500 nm pillars separated by 500 nm; (b) 140 nm pillars separated by 90 nm.

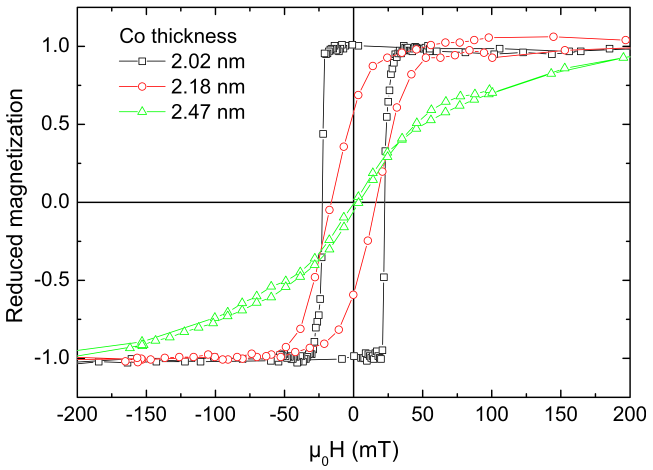

FIG. 2. EHE loops with a perpendicular magnetic field for continuous Pt/Co/MgO layers with 2.02, 2.18, and 2.47 nm Co thickness.

while $K_V = (1.08 \pm 0.1) \times 10^6\,J/m^3$, using the spontaneous magnetization $\mu_0 M_S$ of about 1.76 T measured with SQUID.

In order to investigate the magnetization switching of the pillars, we measured hysteresis loops using the focused Kerr setup. An example is shown for the pillars with 2.47 nm of Co in Fig. 4. These loops were recorded with the coil providing a maximum field of 80 mT, using a field sweep rate of 0.35 T/s. For this thickness, the coercivity and remanence are low for the large pillars, while loops with full remanence and high coercivity are found for pillar sizes smaller than 100 nm. In order to check if the small opening of the loops for the largest pillars, which is absent in the EHE loops for the same Co thickness, was due to dynamic effects induced by the relatively high field sweep rates used in the Kerr measurements, we recorded hysteresis loops for field sweep rates between 0.17 T/s and 7 T/s for the 2 μm and 140 nm pillars. No significant changes were observed below 0.7 T/s. The small remanence is thus likely to be related to a small perpendicular component of the magnetization of the pillars, probably at the edges of the pillars. For the 30, 60, and 140 nm pillars, small differences in the shape of the hysteresis loops were observed for arrays with different pillar spacings, probably due to dipolar interactions between the pillars.

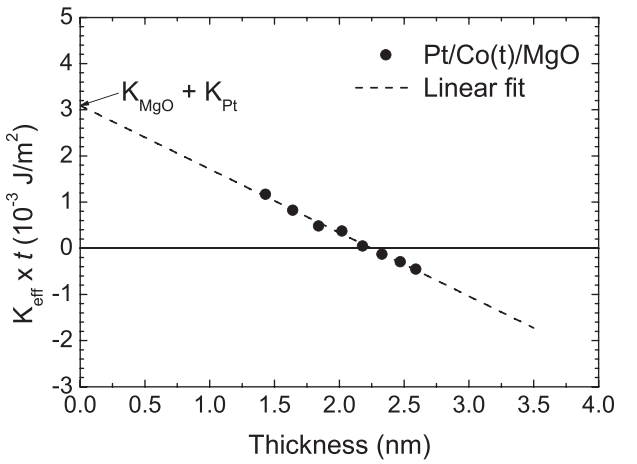

FIG. 3. $K_{eff} \times t$ as a function of Co thickness t. The straight line is a linear fit to the data.

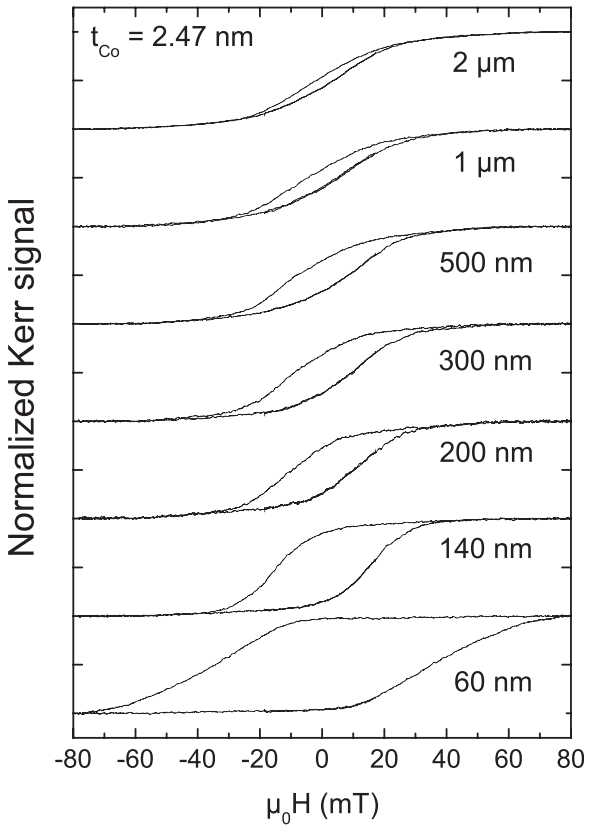

FIG. 4. Kerr hysteresis loops for 2.47 nm Co thickness, for different pillar sizes.

However, these interactions did not significantly influence the coercive fields.

In Fig. 5, we show the measured coercivities for all Co thicknesses and pillar sizes. The points for the three largest Co thicknesses (2.33, 2.47, and 2.59 nm) were measured using the coil with low remanence, at a field sweep rate of 0.35 T/s, except for the smallest pillars, with a coercivity larger than 40 mT. These points, as well as all the points for the 1.84, 2.02, and 2.31 nm thick Co layers, were measured with the coil providing a higher field, at a field sweep rate of 0.55 T/s. For all Co thicknesses, the coercive field increases with decreasing pillar size. In a first approximation, the trends of the coercivities as a function of pillar size can be compared to the variation of the out-of-plane demagnetizing factor N_z.[19] The reduction of N_z as the pillar size decreases follows the same trend as the coercivity, as can be seen in Fig. 5. Indications that demagnetizing effects are at the origin of the size dependence of the coercivity were also found directly from the hysteresis loops for the larger (>500 nm) pillars with a Co thickness close to the spin reorientation transition (2.02, 2.18, and 2.33 nm). For these pillars, the measured coercive field depended on the position of the laser spot and often two coercivity steps were observed. This was the case even for the 2 μm pillars, which are larger than the laser spot size. The lowest coercivity was found where the reflectivity was the highest, suggesting that the magnetization switching starts in the center of the pillars, where the demagnetizing field is the largest, while the borders switch at higher fields through propagation of the domain walls formed in the center.

The demagnetizing factors according to Aharoni[19] suppose a homogeneous magnetization inside the pillars. However, for values of $K_{eff} \sim 0$, the magnetization configuration is not expected to be homogeneous, especially during switching.[20,21] In order to take the variation of the demagnetizing field over the pillar surface into account, we performed micromagnetic simulations using the Micro3D software.[22] Spontaneous magnetization and anisotropy constants were taken from the experimental results. A magnetic stiffness of 30 pJ/m was used.[23] The damping parameter value was set to 0.5. The simulations were performed at 0 K by starting from negative saturation, then reversing the direction of the field and increasing its amplitude in steps of 5 mT. The field was applied with a small angle of 0.5° with respect to the easy (perpendicular) magnetization axis. For each field value, we waited until the energy minimum was reached (residual torque $m \times H_{eff}/M_s < 10^{-6}$) before increasing its value. Fig. 6

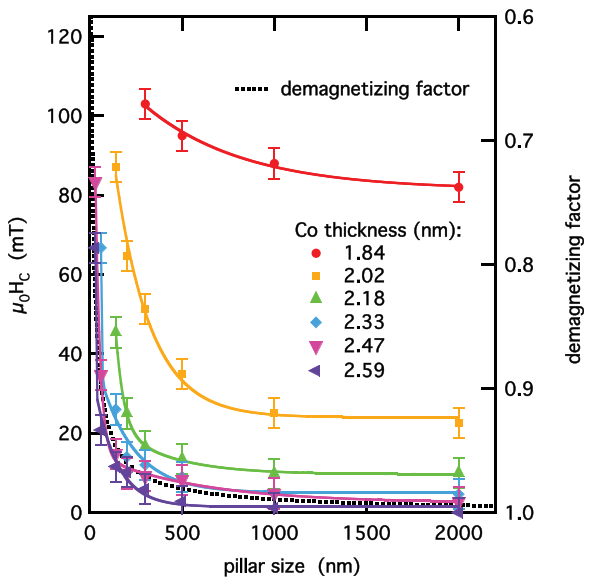

FIG. 5. Coercivity as a function of pillar size (left axis), for different Co thickness. The continuous lines are guides for the eye. The perpendicular demagnetizing factor N_z as a function of pillar size, for a Co thickness of 2.47 nm, is also given (right axis)

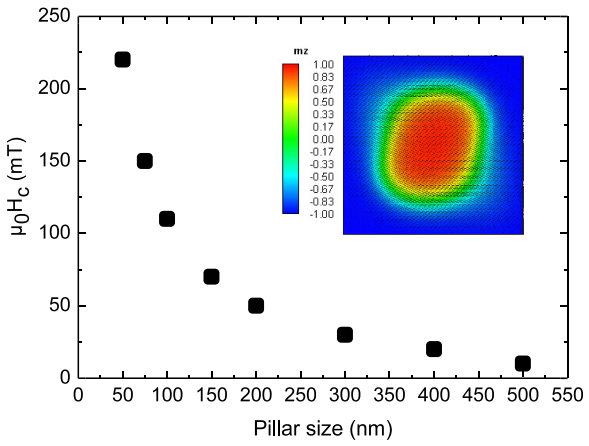

FIG. 6. Coercivity as a function of pillar size for 2.18 nm of Co, with $K_{eff} = 0.9 \times 10^4$ J/m^3, obtained using micromagnetic simulations. The inset shows the square 300×300 nm^2 pillar in an intermediate state during magnetization reversal from down to up. The color code indicates the m_z component of the magnetization, red (intermediate grey) for up and blue (dark grey) for down.

gives the results, corresponding to the quasi-static switching fields, as a function of pillar size, for 2.18 nm of Co, i.e., just below the spin reorientation transition in the continuous films. For this Co thickness, the single-domain state is the most stable one at zero field, at least for lateral sizes smaller than 500 nm. Upon switching, the magnetization reversal starts in the center where the demagnetizing field is largest, except for the smallest pillars ($\leq$60 nm) where the switching is almost coherent. An example is shown for pillars of 300 nm in the inset of Fig. 6. Upon switching from down to up in a magnetic field of 40 mT, a bi-domain state with magnetization up in the center and down at the edge of the pillar is formed, followed by propagation of the domain walls towards the borders. The results of the simulations reproduce the experimental trend, confirming the crucial influence of the demagnetizing field on the magnetization switching in our pillars.

For Co thicknesses of 2.33, 2.47, and 2.59 nm, the remanence and coercivity for the larger pillars are almost zero, indicating in-plane magnetization. Upon going to smaller pillars, both remanence and coercivity increase until the remanence is 100%. This occurs for pillar sizes of 200, 140, and 60 nm for Co thicknesses of 2.33, 2.47, and 2.59 nm, respectively.

In conclusion, we have performed systematic studies of the magnetization switching of submicrometer sized pillars fabricated from MgO/Co/Pt layers with different Co thicknesses around the transition from out-of-plane to in-plane magnetization. We observed experimentally that the coercive field strongly increases with decreasing pillar size for all Co thicknesses. Full perpendicular remanence and high coercivities (above 40 mT) were observed for sub-100 nm pillars even for Co thicknesses for which the magnetization was in-plane in continuous layers. The observed trends are in good quantitative agreement with micromagnetic simulations using the experimental parameters for bulk and interface magnetic anisotropies obtained from measurements on the continuous layers. The main origin of the increase in coercivity upon decreasing size is thus the increase of the effective perpendicular anisotropy due to changes in magnetostatic effects, while defects seem to play a minor effect, contrary to what was observed for materials with strong PMA, where the influence of demagnetizing effects is smaller.[4,6,24–26] The optimization of the effective PMA by tuning the thickness of the magnetic layer and the size of the pillar is useful to find the optimum trade-off between thermal stability and critical current density for STT switching.[14,15]

We acknowledge the Laboratory of Cryogenic and Spintronic Research in the Institute of Physics PAS (Warszawa, Poland) for access to the SQUID magnetometer. We thank O. Fruchart for Magnetic Force Microscopy measurements. This work was supported by the Agence National de la Recherche through the project ANR-10-NANO PATHOS. W.K. thanks the DAAD for a Grant (Project ID 55985924).

[1]S. Monso, B. Rodmacq, S. Auffret, G. Casali, F. Fettar, B. Gilles, B. Dieny, and P. Boyer, Appl. Phys. Lett. **80**, 4157 (2002).
[2]S. Ikeda, K. Miura, H. Yamamoto, K. Mizunuma, H. Gan, M. Endo, S. Kanai, J. Hayakawa, F. Matsukura, and H. Ohno, Nature Mater. **9**, 721 (2010).
[3]J. Moritz, B. Dieny, J. Nozieres, R. van de Veerdonk, T. Crawford, D. Weller, and S. Landis, Appl. Phys. Lett. **86**, 063512 (2005).
[4]J. M. Shaw, S. E. Russek, T. Thomson, M. J. Donahue, B. D. Terris, O. Hellwig, E. Dobisz, and M. L. Schneider, Phys. Rev. B **78**, 024414 (2008).
[5]M. Abes, M. V. Rastei, J. Venuat, A. Carvalho, S. Boukari, E. Beaurepaire, P. Panissod, A. Dinia, J. P. Bucher, and V. Pierron-Bohnes, J. Appl. Phys. **105**, 113916 (2009).
[6]T. Seki, H. Iwama, T. Shima, and K. Takanashi, J. Phys. D: Appl. Phys. **44**, 335001 (2011).
[7]T. Bublat and D. Goll, J. Appl. Phys. **110**, 073908 (2011).
[8]H. Wang, M. T. Rahman, H. Zhao, Y. Isowaki, Y. Kamata, A. Kikitsu, and J.-P. Wang, J. Appl. Phys. **109**, 07B754 (2011).
[9]B. Rodmacq, S. Auffret, B. Dieny, S. Monso, and P. Boyer, J. Appl. Phys. **93**, 7513 (2003).
[10]J. Z. Sun, R. P. Robertazzi, J. Nowak, P. L. Trouilloud, G. Hu, D. W. Abraham, M. C. Gaidis, S. L. Brown, E. J. O'Sullivan, W. J. Gallagher, and D. C. Worledge, Phys. Rev. B **84**, 064413 (2011).
[11]H. Sato, M. Yamanouchi, K. Miura, S. Ikeda, H. D. Gan, K. Mizunuma, R. Koizumi, F. Matsukura, and H. Ohno, Appl. Phys. Lett. **99**, 042501 (2011).
[12]M. Gajek, J. J. Nowak, J. Z. Sun, P. L. Trouilloud, E. J. O'Sullivan, D. W. Abraham, M. C. Gaidis, G. Hu, S. Brown, Y. Zhu, R. P. Robertazzi, W. J. Callagher, and D. C. Worledge, Appl. Phys. Lett. **100**, 132408 (2012).
[13]J. W. Chenchen, M. A. K. B. Akhtar, R. Sbiaa, M. Hao, L. Y. H. Sunny, W. S. Kai, L. Ping, P. Carlberg, and A. K. S. Arthur, Jpn. J. Appl. Phys., Part 1 **51**, 013101 (2012).
[14]M. T. Rahman, A. Lyle, P. K. Amiri, J. Harms, B. Glass, H. Zhao, G. Rowlands, J. A. Katine, J. Langer, I. N. Krivorotov, K. L. Wang, and J. P. Wang, J. Appl. Phys. **111**, 07C907 (2012).
[15]H. Meng, R. Sbiaa, S. Y. H. Lua, C. C. Wang, M. A. K. Akhtar, S. K. Wong, P. Luo, C. J. P. Carlberg, and K. S. A. Ang, J. Phys. D: Appl. Phys. **44**, 405001 (2011).
[16]B. Rodmacq, A. Manchon, C. Ducruet, S. Auffret, and B. Dieny, Phys. Rev. B **79**, 024423 (2009).
[17]L. E. Nistor, B. Rodmacq, S. Auffret, and B. Dieny, Appl. Phys. Lett. **94**, 012512 (2009).
[18]L. E. Nistor, Ph.D. dissertation, Université de Grenoble, 2011.
[19]A. Aharoni, J. Appl. Phys. **83**, 3432 (1998).
[20]A. Maziewski, V. Zablotskii, and M. Kisielewski, Phys. Rev. B **73**, 134415 (2006).
[21]T. Polyakova, M. Kisielewski, A. Maziewski, and V. Zablotskii, J. Appl. Phys. **103**, 073912 (2008).
[22]L. D. Buda, I. L. Prejbeanu, U. Ebels, and K. Ounadjela, Comput. Mater. Sci. **24**, 181 (2002).
[23]G. Shirane, V. J. Minkiewicz, and R. Nathans, J. Appl. Phys. **39**, 383 (1968).
[24]T. Thomson, G. Hu, and B. D. Terris, Phys. Rev. Lett. **96**, 257204 (2006).
[25]T. Seki, T. Shima, K. Yakushiji, K. Takanashi, G. Q. Li, and S. Ishio, J. Appl. Phys. **100**, 043915 (2006).
[26]J. M. Shaw, M. Olsen, J. W. Lau, M. L. Schneider, T. J. Silva, O. Hellwig, E. Dobisz, and B. D. Terris, Phys. Rev. B **82**, 144437 (2010).